

# High-latitude dust deposition in snow on the glaciers of James Ross Island, Antarctica

Jan Kavan,<sup>1\*</sup>  Daniel Nývlt,<sup>1</sup> Kamil Láska,<sup>1</sup> Zbyněk Engel<sup>2</sup> and Michaela Kňázková<sup>1</sup>

<sup>1</sup> Polar-Geo-Lab, Department of Geography, Faculty of Science, Masaryk University, Kotlářská 2, CZ-611 37 Brno, Czech Republic

<sup>2</sup> Department of Physical Geography and Geocology, Faculty of Science, Charles University in Prague, Albertov 6, CZ-128 42 Prague, Czech Republic

Received 19 February 2019; Revised 27 January 2020; Accepted 27 January 2020

\*Correspondence to: Jan Kavan, Polar-Geo-Lab, Department of Geography, Faculty of Science, Masaryk University, Kotlářská 2, CZ-611 37 Brno, Czech Republic.  
E-mail: jan.kavan.cb@gmail.com

# ESPL

Earth Surface Processes and Landforms

**ABSTRACT:** High-latitude dust (HLD) depositions on four glaciers of James Ross Island (the Ulu Peninsula) were analysed. The deposition rate on the selected glaciers varies from 11.8 to 64.0 g m<sup>-2</sup>, which is one order of magnitude higher compared to the glaciers in Antarctica or elsewhere in the world. A strong negative relationship between the sediment amount and altitude of a sampling site was found. This is most likely caused by the higher availability of aeolian material in the atmospheric boundary layer. General southerly and south-westerly wind directions over the Ulu Peninsula – with exceptions based on local terrain configuration – help to explain the significantly lower level of sediment deposition on San Jose Glacier and the high level on Triangular Glacier. X-ray fluorescence (XRF) spectrophotometry was used to estimate the relative proportions of the main and trace (lithophile) elements in the sediment samples. Both the sediment amount and the XRF results are analysed in a depth profile at each locality and compared among the glaciers, suggesting long-range transport of fine mineral material from outside James Ross Island. The distribution of aeolian sediment among the glaciers corresponds well with the prevailing wind direction on the Ulu Peninsula. © 2020 John Wiley & Sons, Ltd.

**KEYWORDS:** glaciers; high-latitude dust deposition; snow pit; James Ross Island; Antarctic Peninsula; long-range transport

## Introduction

Glaciers and snowfields are important areas where wind-transported material is deposited. They serve both as storage and an important amount of sediment material is also released from their body (Atkins and Dunbar, 2009). Glacier surfaces are often the source of sediment material for proglacial rivers (Fortner *et al.*, 2011; Bullard, 2013). The redistribution of mineral material throughout the glacial system is presently understudied (Bullard *et al.*, 2016). Previous Antarctic studies dealing with aeolian material were localized to only a few Antarctic areas, mostly the McMurdo Dry Valleys (e.g. Selby *et al.*, 1974; Ayling and McGowan, 2006; Speirs *et al.*, 2008; Fortner *et al.*, 2011; Šabacká *et al.*, 2012) and some sub-Antarctic islands (Hedding *et al.*, 2015). The importance of HLD sources is still not fully acknowledged. The redistribution of aeolian and fluvial material is studied, for example, in Greenland (Bullard and Austin, 2011) and other Arctic areas (e.g. Arnalds *et al.*, 2013, 2016; Croft *et al.*, 2016). The first attempt to deal with the provenance of fluvial material on James Ross Island was presented in Kavan *et al.* (2017) and a possible source of the fluvial material from aeolian transport was identified and tested using aeolian passive samplers in the braidplain of the Bohemian Stream (Kavan and Nývlt, 2018). It was shown that approximately 30% of the wind-transported material is deposited in the braidplain and subsequently transported by

fluvial processes. Atmospheric conditions leading to the activation of local dust sources are predisposed, especially with a wind speed of >10 m s<sup>-1</sup>. These wind speeds trigger the uplift of local surface material – particles larger than 5 µm. Mostly, such conditions occur during the episodes of barrier winds flowing from the south to the south-west. Apart from local dust sources (on the scale of up to tens of square kilometres), long-range transport from the Patagonian desert areas was also recorded in February 2018 (Kavan *et al.*, 2018; Gassó and Torres, 2019). The impact of wind-induced dust/snow deposition on small-scale landforms on the Ulu Peninsula was described in Kňázková *et al.* (2020).

We know relatively little about the spatial and temporal variability of the chemical composition of dust (Lawrence and Neff, 2009). Even less is known about deposition on Antarctic glaciers. Trace elements deposited by wind were studied only on the surface of Taylor Valley glaciers by Fortner *et al.* (2011) and by Bory *et al.* (2010) on the Berkner Island ice sheet, while other works focused on the Antarctic Peninsula (Pereira *et al.*, 2004). However, the issue of the chemical composition of aeolian deposition in Antarctica is frequently addressed in paleoenvironmental studies (Basile *et al.*, 1997; Delmonte *et al.*, 2004; Fischer *et al.*, 2007). The chemical composition of Antarctic snow in the Ross Sea sector was evaluated in Dixon *et al.* (2013), identifying both a regional volcanic source (Mt Erebus) and long-range sources of the deposited material.

More attention has been directed towards the chemical composition of ice cores (e.g. Vallelonga *et al.*, 2004) where volcanic and anthropogenic inputs are evaluated throughout the ice core record. The provenance of the deposited dust in Antarctica is usually attributed to a source area in Patagonia (Fischer *et al.*, 2007; Gassó *et al.*, 2010; Gassó and Torres, 2019) or to South America in general (Gaiero, 2007; Gilli *et al.*, 2016). The characteristics of sea salt aerosol were studied at Neumayer Station (Weller *et al.*, 2008) and Concordia Research Station (Legrand *et al.*, 2017). Black carbon concentrations are monitored on a long-term basis at Neumayer Station (Weller *et al.*, 2013).

In this study, the aeolian deposition on four glaciers on the Ulu Peninsula, James Ross Island, was examined. A quantitative evaluation of the sediment amount is discussed with respect to the local topographic and surface wind conditions. The amounts of the main and trace elements were estimated and local/long-range sources are identified based on this.

## Study Area

The northern part of James Ross Island, the Ulu Peninsula (312 km<sup>2</sup>), is the largest ice-free area in the Antarctic Peninsula region (Kavan *et al.*, 2017). Nevertheless, a number of small glaciers are located in the area (Rabassa *et al.*, 1982), and some of them have been the subject of detailed studies (e.g. Engel *et al.*, 2012). Some of these glaciers experienced a surface mass gain over the period 2009–2015 of  $0.57 \pm 0.67$  and  $0.11 \pm 0.37$  m w.e. on Whisky Glacier and Davies Dome, respectively

(Engel *et al.*, 2018). Four glaciers were chosen to estimate the amount of aeolian material input to their surface, and to characterize its mineral composition and provenance. The important role of snow redistribution on the spatial pattern of mass balance was identified on a few glaciers on the Ulu Peninsula (Láska *et al.*, 2017; Engel *et al.*, 2018).

The locations of the four investigated glaciers (Davies Dome, Whisky Glacier, Triangular Glacier, San Jose Glacier), together with the position of the snow pits and automatic weather stations (AWS), are illustrated in Figure 1. The glaciers differ in their areal extent, elevation and orientation. The typology of the selected glaciers also presents a notable difference. While Davies Dome is considered to be a dome-type glacier, the other glaciers are of valley type. The basic glacier characteristics are summarized in Table I. The orientation of the glaciers is also quite different – Whisky Glacier is oriented towards the north, Triangular Glacier towards the west and San Jose towards the south. Davies Dome as a dome-type glacier is not specifically oriented, nevertheless the altitude profile on Davies Dome consisting of three snow pits is oriented towards the north.

## Materials and Methods

### Snow and sediment sampling

Snow pits for material sampling were dug in the accumulation zones of the glaciers during February 2018. Even though all the snow pits are located in the accumulation area of the glaciers,

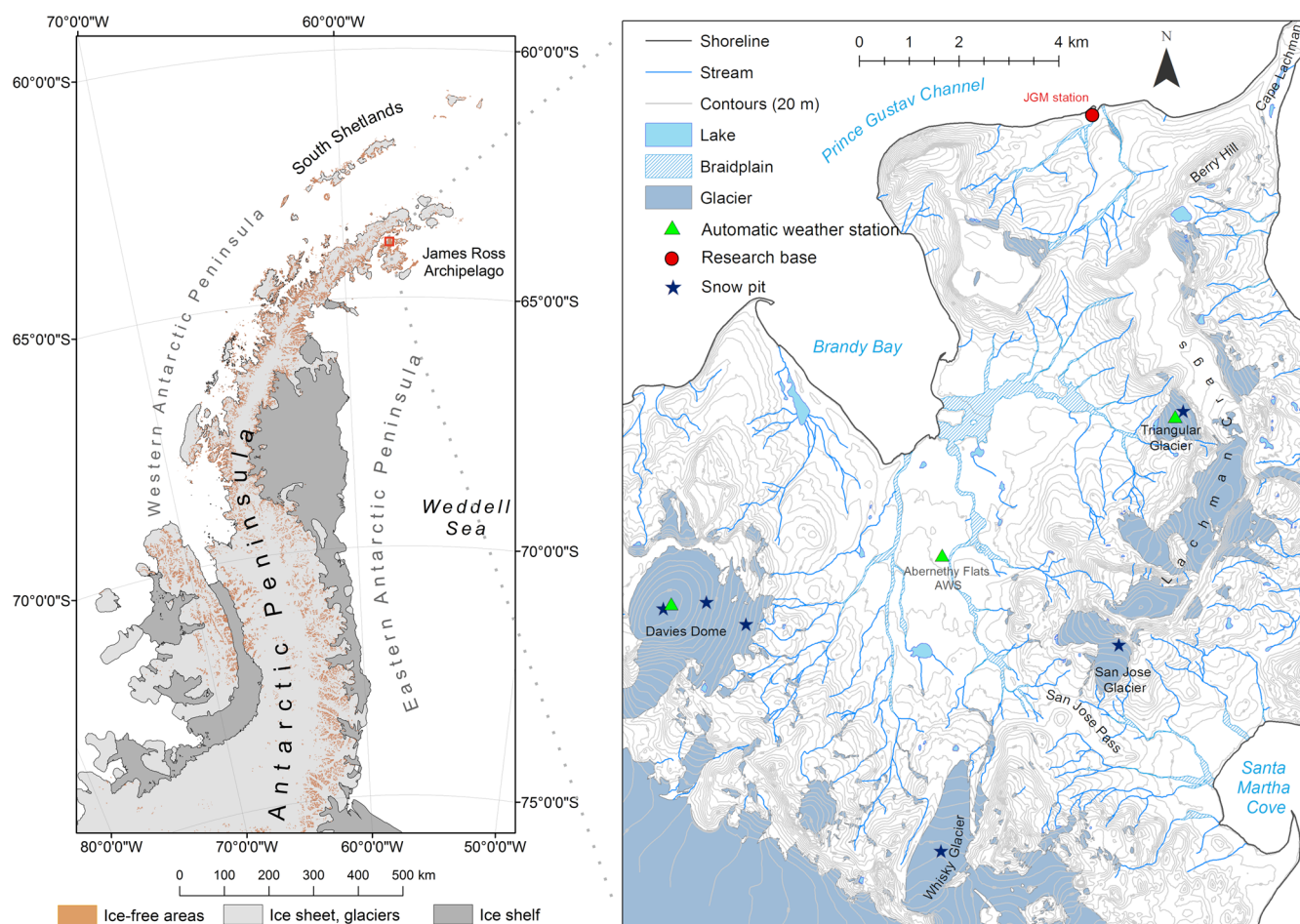


**Figure 1.** Study site location within the Antarctic Peninsula region; Ulu Peninsula with AWS, snow pits and general topography of the area. [Colour figure can be viewed at [wileyonlinelibrary.com](http://wileyonlinelibrary.com)]

**Table I.** Studied glacier characteristics and basic sampling parameters.

Glacier	San Jose Glacier	Triangular Glacier	Whisky Glacier	Davies Dome
Sampling date	30.1.2018	14.2.2018	9.2.2018	19.2.2018
Sampling altitude (m a.s.l.)	265	210	350	510/430/270
Glacier area (km <sup>2</sup> )	0.61	0.59	2.34	6.67
Average glacier altitude (m a.s.l.)	220	185	330	400
Minimum glacier altitude (m a.s.l.)	140	110	220	0
Maximum glacier altitude (m a.s.l.)	300	310	460	510

they differ significantly in altitude. All were dug down to the glacier ice surface. The snow was sampled with a plastic tube of 5 cm diameter and was sampled from the distinctive snow layers (i.e. with variable snow depths, to keep the layer as homogeneous as possible). The total depth of the snow pits varied from 91 cm on the Triangular Glacier to 33 cm on Davies Dome (the lower site near the equilibrium line). The snow pits and sediment sample characteristics (depths and density) are summarized in Table II. The snow samples were stored in plastic zip-lock bags and transported immediately to the laboratory facility at Johann Gregor Mendel (JGM) Station. After the samples had melted, they were filtered with the pre-weighed Whatman 0.45- $\mu\text{m}$  filters, dried in a SNOL 120/300 LSN11 laboratory oven at 40°C and the filters with the sediments were weighed (with a precision of 0.0001 g) and stored in plastic zip-lock bags. The samples were kept at room temperature and transported to the Polar-Geo-Lab (Masaryk University, Brno, Czechia) for subsequent analyses.

The total sediment content measured in the snow pits on Davies Dome and Whisky Glacier (Table II) was used to determine the vertical deposition gradient based on linear regression. The same gradient is assumed for San Jose and Triangular Glacier, where the sediment content was determined only in one elevation. The measured sediment content differs from the linear fit by  $-14.36$  and  $35.19 \text{ g m}^{-2}$  for San Jose Glacier and Triangular Glacier, respectively (Figure 2). The sediment deposition was distributed over the glacier surfaces following the obtained deposition gradient and the respective shift in the deposition value. The mean deposition rate was determined from the deposition grid obtained for each glacier. The total sediment content on the glaciers was calculated by multiplying the mean deposition rate corresponding to its mean altitude and the glacier surface area (Table I).

## X-ray fluorescence assessment of main and trace elements

All samples were processed to assess the relative proportions of main and trace (lithophile) elements by means of X-ray fluorescence (XRF) spectrophotometry. XRF measurements of dried sediments were conducted using a portable Innov-X System DELTA analyser. Each sample was analysed three times for a 90-s measurement period in the soil-geochem mode. These three measurements were averaged and the average values were used in further analyses. The relative proportions of the selected elements (Al, Si, K, Ca, Ti, Fe, Rb, Sr) and important ratios (Al/Si, K/Ca, Sr/Ca, Rb/Sr, Fe/Ti) were used to assess the chemical composition of the sediments, as well as the environmental and geological provenance of the material. Some of the elements were under the limit of detection (<LOD) of the measurement device, pointing to very low concentrations in general. On the contrary, highly soluble ions, such as  $\text{Cl}^-$ ,  $\text{ClO}_3^-$  and  $\text{SO}_4^{2-}$ , were not taken into account as most of their content remained dissolved in the liquid phase after filtering and their relative proportions are therefore under-represented. The results were validated by the analysis of certified reference material CH-4 (Natural Resources Canada), because of the similar proportions of the main elements and most of the trace elements analysed both in the snow samples as well as in the background geological samples (volcanic and sedimentary rocks). The comparison of XRF-based trace element proportions and elemental ratios with ICP-based geochemical data from James Ross Island Volcanic Group (JRIVG) basaltic rocks (Kořler et al., 2009; Altunkaynak et al., 2018) proved the suitability of the XRF spectrophotometry for our study. Replicate measurements of the same sample showed differences of <1% for all assessed elements.

**Table II.** Snow pit sediment amount parameters.

Glacier	San Jose Glacier		Triangular Glacier		Whisky Glacier	
	Depth (cm)	Material ( $\text{g m}^{-2}$ )	Depth (cm)	Material ( $\text{g m}^{-2}$ )	Depth (cm)	Material ( $\text{g m}^{-2}$ )
Vertical profile	76–82	0.66	73–91	6.06	68–77	5.86
	59–76	2.19	50–73	52.97	60–68	6.37
	45–59	1.43	32–50	4.79	40–60	5.14
	37–45	2.70	0–32	0.20	24–40	2.55
	0–37	4.84			0–24	0.76
Total sediment amount ( $\text{g m}^{-2}$ )	11.82		64.02		20.68	
Total snow profile depth (cm)	82		91		77	
Glacier	Davies Dome (top)		Davies Dome (middle)		Davies Dome (down)	
Vertical profile	Depth (cm)	Material ( $\text{g m}^{-2}$ )	Depth (cm)	Material ( $\text{g m}^{-2}$ )	Depth (cm)	Material ( $\text{g m}^{-2}$ )
	49–34	4.94	58–42	4.18	33–0	26.50
	34–17	4.99	42–28	4.99		
	17–0	4.79	28–7	4.58		
	7–0		7–0	4.63		
Total sediment amount ( $\text{g m}^{-2}$ )	14.72		18.39		26.50	
Total snow profile depth (cm)	49		58		33	

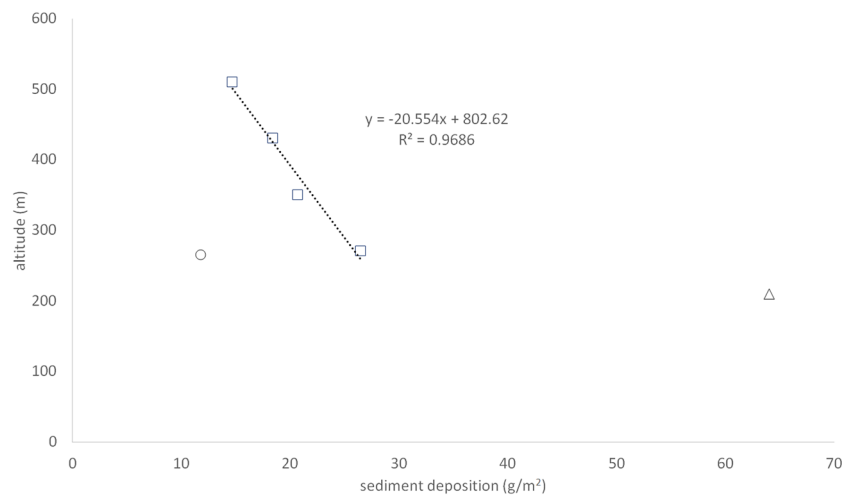


**Figure 2.** Relation between the snow pit altitude and sediment deposition; San Jose glacier is marked with a circle, Triangular glacier with a triangle, the other sampling sites with squares. [Colour figure can be viewed at [wileyonlinelibrary.com](http://wileyonlinelibrary.com)]

### Estimation of prevailing wind directions

The surface wind direction and wind speed measurements were obtained from AWS installed on Davies Dome, Triangular Glacier and Abernethy Flats. The wind components were measured with the same 05108 Young Heavy Duty Wind Monitor (R. M. Young Co., Michigan, WI), with a threshold sensitivity of  $1.0 \text{ m s}^{-1}$  for both output parameters. Sampling and recording intervals were set every 30 min and data were stored in an EdgeBox V12 datalogger (EMS, Czechia). The heights of the wind instruments were 2.0–2.2 m above the surface of Davies Dome and Triangular Glacier AWS, and 3.0 m above the ground at the Abernethy Flats station. Observation records were available for the period from 1 February 2017 to 31 January 2018. The variability of the wind parameters was analysed and visualized with Grapher 13 software for 16 directional sectors of a wind rose diagram.

Apart from these wind direction records, aerial photographs (1979, 2006), satellite images (2013, 2017), terrestrial photographs (2017, 2018) and field observations were used to estimate the prevailing wind directions on the Ulu Peninsula. Volcanic boulders and other terrain elevations create an obstacle to the wind flow and determine the position of snow accumulation in the area. The prevailing wind direction conditions were therefore estimated on the basis of snow accumulation around the distinct terrain features (e.g. volcanic boulders). A total of 69 wind direction points were determined and a map of the prevailing wind direction on the Ulu Peninsula was created (Figure 3).

### HLD deposition in directional passive sampler

A passive aeolian sediment sampler was installed near the AWS at Abernethy Flats. It was deployed for approximately 2 months and collected after the first period (28 January–28 February 2018) and second period (28 February–22 March 2018). The passive sampler was constructed to catch the aeolian surface sediment flux in 24 angle sectors ( $15^\circ$ ). The samples were washed from the collectors and the amount of trapped sediment was determined in the lab at JGM Station. The samples were filtered using pre-weighed Whatman 3- $\mu\text{m}$  filter paper and subsequently dried in a SNOL 120/300 LSN11 laboratory oven at  $40^\circ\text{C}$  for 48 h and weighed (with a precision of 0.0001 g).

## Results

### High-latitude dust deposition

The amount of HLD found on the selected glaciers varies between  $11.8$  and  $64 \text{ g m}^{-2}$ . A strong correlation between the amount of aeolian material and altitude can be found in the set of all snow pits apart from San Jose Glacier, which does not fit in the relationship (Figure 2). The lowest sediment concentration (apart from San Jose Glacier) is found on top of Davies Dome ( $14.7 \text{ g m}^{-2}$ ), which is the highest sampling locality. There were five well-distinguished snow layers identified on the Whisky, San Jose and Triangular glaciers, whereas only three were identified and sampled on Davies Dome. Vertical profiles through the snow pits reveal that the largest amount of sediment is concentrated in the second highest layer, around a depth of 20 cm in the case of Whisky and Triangular glaciers. San Jose Glacier exhibits a contradictory pattern with the maximum concentrations in the bottom layer, whereas Davies Dome has relatively homogeneous sediment concentrations throughout the whole depth profile (Figure 4).

The calculation of sediment amount based on the altitude/sediment deposition relation (Figure 2) and glacier parameters – area and mean altitude (Table I) – reveals the total amount of sediment stored in the snow on the glacier surface. It has to be pointed out that the calculation is typically based on a single snow pit (except Davies Dome), and is therefore rather informative. A total of 139.2 tons of HLD is stored in the Davies Dome surface snow, 53.2 tons in Whisky Glacier, 37.7 tons in Triangular Glacier and only 8.5 tons in San Jose Glacier.

### Main and trace element proportions and elemental ratios

To reveal the chemical composition of the sediments, as well as their environmental and lithological provenance, the main and trace elements and their ratios were studied in all the samples using XRF spectrophotometry. The proportions of the basic elements for the investigated glaciers are summarized in Table III, and their vertical profile illustrated in Figure 5. These data were compared with the elemental composition of principal bedrock lithologies (Figure 6). The studied elements (Al, Si, K, Ca, Ti, Fe, Rb, Sr) have the highest contents in the sediment samples from

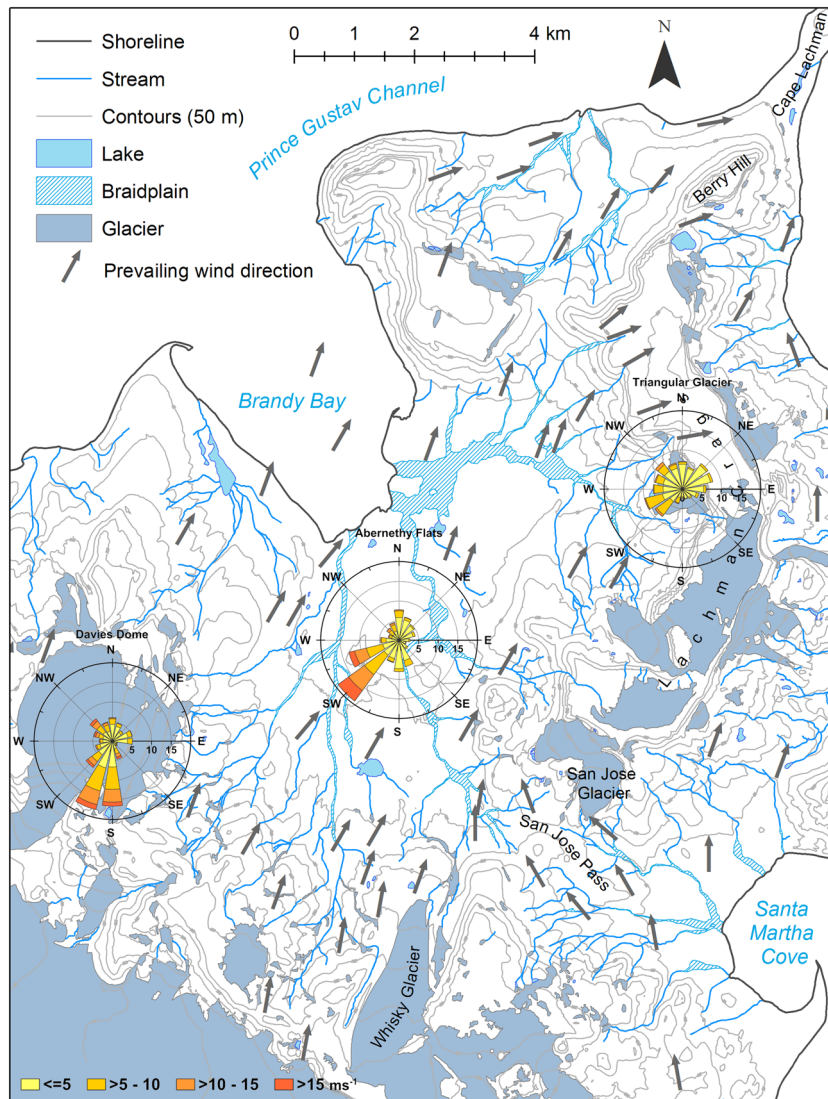


**Figure 3.** Prevailing wind directions derived from boulders and similar terrain features on the Ulu Peninsula together with wind roses at the three AWS. [Colour figure can be viewed at [wileyonlinelibrary.com](http://wileyonlinelibrary.com)]

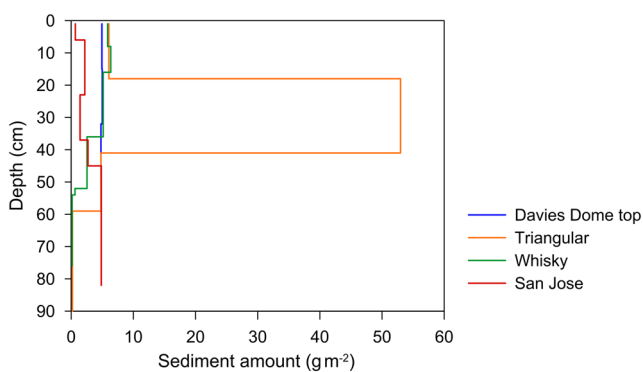


**Figure 4.** Sediment amount in the snow profile of the studied glacier. [Colour figure can be viewed at [wileyonlinelibrary.com](http://wileyonlinelibrary.com)]

Triangular Glacier and Davies Dome – down, sample and generally lower contents in sediments collected from the other glaciers.

Similarly, the calculated ratios (Table IV) clearly separate the samples collected on San Jose and Whisky glaciers and Davies Dome top site (high Al/Si and Rb/Sr ratios) from the samples obtained for Triangular Glacier and Davies Dome down sites (high Sr/Ca, K/Ca and particularly Fe/Ti ratios and vice versa, see Table IV). Especially the high K/Ca and lower Sr/Ca indices

are similar to Santa Marta Fm. bedrock, rather than to JRIVG basalts and hyaloclastites, for which negligible Rb/Sr index is typical (Table IV, Figure 6).

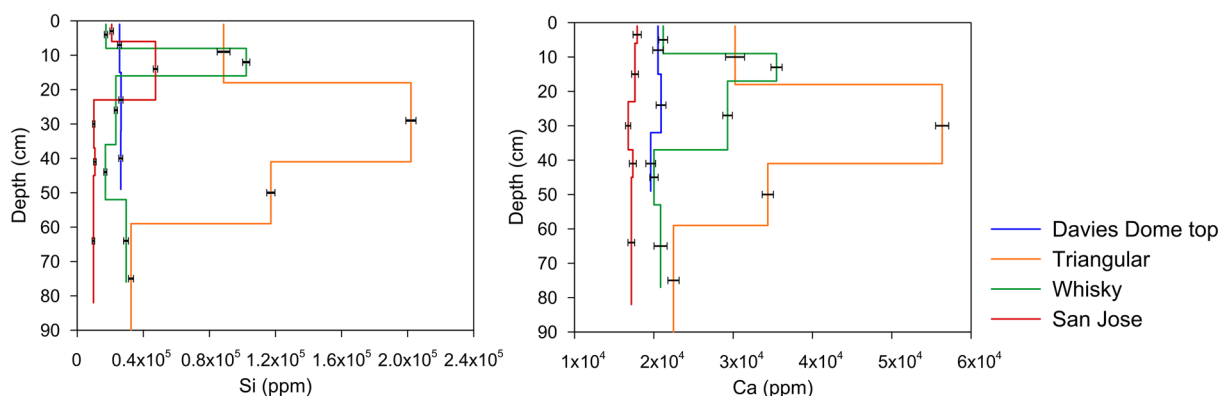
### Prevailing wind direction and HLD transport

The dominant wind direction on the Ulu Peninsula is south-westerly, driven by the strong barrier winds, as shown in Figure 3. However, local differences in wind direction were identified, especially in the area of San Jose Pass, where the wind is strongly deflected by local topography. Prevailing winds flow from Santa Martha Cove towards the San Jose Pass (south-easterly direction), avoiding the massif of Lachman Crags. A similar, but not so strong, effect of the local terrain was identified along the eastern coast of the Ulu Peninsula between Santa Martha Cove and Cape Lachman (south to south-easterly direction), and in the area of Triangular Glacier (west to south-westerly), where the wind flows over the Lachman Crags. Moreover, the western winds were observed at the northern and southern slopes of Berry Hill.

The strong influence of the local topography of the Ulu Peninsula on the surface wind pattern is also apparent from the AWS observations (Figure 3). Based on the yearly data, the most frequent directions corresponded to southerly and south-

**Table III.** Proportions of main and trace elements (ppm) in snow pits; proportions of some of the elements were under the detection limit (blank spaces).

Glacier/snow pit	Al	Si	K	Ca
San Jose	17446 ± 2589	19792 ± 807	8959 ± 352	17358 ± 374
Whisky	24948 ± 2542	37945 ± 1191	11749 ± 439	25360 ± 583
Triangular	27022 ± 2523	110116 ± 2649	21499 ± 623	35859 ± 804
Davies Dome (top)		26185 ± 1128	10230 ± 471	20345 ± 572
Davies Dome (down)		63110 ± 1994	15431 ± 560	24165 ± 687
Glacier/snow pit	Ti	Fe	Rb	Sr
San Jose	5009 ± 215	1603 ± 51	4.853 ± 1.305	6.904 ± 1.290
Whisky	11279 ± 341	3090 ± 86	4.75 ± 1.310	7.772 ± 1.364
Triangular	7005 ± 284	27850 ± 487	20.723 ± 2.277	49.854 ± 2.538
Davies Dome (top)		1378 ± 56		6.746 ± 1.444
Davies Dome (down)	1650 ± 169	9621 ± 266	4.52 ± 1.515	13.357 ± 1.600

**Figure 5.** Relative contents of main elements in the snow profiles (Si, Ca). [Colour figure can be viewed at [wileyonlinelibrary.com](http://wileyonlinelibrary.com)]

westerly winds. Mean occurrence frequencies of the winds were 30.4% (Davies Dome) and 36.8% (Abernethy Flats), of all the cases. The strongest winds ( $>15 \text{ m s}^{-1}$ ) were found with frequency of 1.8 and 3.2% during south-westerly flow. In contrast, easterly and south-easterly winds occurred rarely at these sites, with a total frequency of  $<5\%$ . The influence of local topography can clearly be seen on Triangular Glacier, where the prevailing wind directions were mainly limited between south-western, north-western and north-eastern sectors. The strongest wind came from north-westerly directions, although the wind speed never exceeded  $15 \text{ m s}^{-1}$  at this site. The general pattern of the prevailing southerly and south-westerly winds obtained from the image analysis and indirect field data corresponds very well with the surface observation mainly at Davies Dome and Abernethy Flats AWS.

The directional passive aeolian sediment sampler confirmed the general trend of prevailing southerly winds in the Abernethy Flats and correspondingly also the transport of aeolian material from the south. The correlation coefficient between wind direction and direction of sediment deposition was 0.55 ( $p < 0.01$ ) for the whole sampling period, only 0.18 (not significant) for the first sampling period, but rather high for the second period – 0.78 ( $p < 0.01$ ).

## Discussion

The data presented in this study suggest that aeolian deposition on the glacier surfaces of James Ross Island might originate mainly from two rather different sources [i.e. (i) from local HLD sources adjacent to the glaciers and (ii) from long-distance sources transporting material in higher levels of the atmosphere]. Our results provide evidence to support this

interpretation for each of the transport mechanisms by (i) clustering the elemental data into two main groups and (ii) the strong negative correlation of altitude and sediment deposition rate on Whisky Glacier and Davies Dome. The first differentiates between the glaciers (Triangular Glacier and the lower part of Davies Dome) on which the local rock fragments (with the dominance of Al, Si, K, Ca, Fe, Rb and Sr) are deposited, and those glaciers (San Jose and Whisky Glacier and the top part of Davies Dome) where mainly long-range-derived material is deposited, which is reflected by lower proportions of elements originating from local bedrock. The latter corresponds with the findings of Lancaster (2002) in McMurdo Dry Valleys for the clay and silt fraction of the deposited material.

The surface wind field over the Ulu Peninsula shows prevailing directions from south to south-west for all the glaciers except San Jose Glacier, which is also the one that differs from the negative relationship of altitude and sediment deposition rate. Winds modified by the local topography come through the San Jose Pass, where its direction is from the east. This causes a relatively small accumulation of aeolian material on San Jose Glacier. The topographically induced wind speed and the direction anomaly are probably also the main reasons for limited snow accumulation on San Jose Glacier, which has experienced the highest surface lowering since the Late Holocene (together with the adjacent Lachman Glacier) among the glaciers studied (Carrivick *et al.*, 2012). In contrast, Triangular Glacier is exposed to southern to south-western winds crossing the ice-free Abernethy Flats (approximately  $15 \text{ km}^2$ ), where much fine-grained loose material from the Cretaceous sedimentary rocks of the Santa Marta Formation and a thin Holocene sedimentary cover (Mlčoch and Nývlt, 2018) is available. Therefore, this glacier receives more than double the amount of HLD that might be expected from the

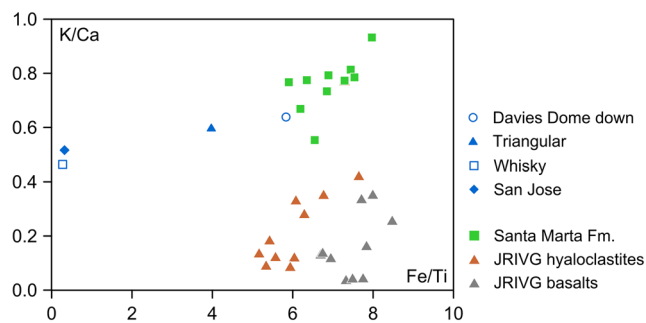


**Figure 6.** Covariant plot of elemental ratio Fe/Ti vs. K/Ca for samples from the studied glaciers (blue and white symbols) compared with the main geological units – sedimentary rocks of Santa Marta Formation (green rectangles), JRIVG hyaloclastite (orange triangles) and JRIVG basalts (grey triangles). [Colour figure can be viewed at [wileyonlinelibrary.com](http://wileyonlinelibrary.com)]

**Table IV.** Elemental ratios of mean and trace elements in snow pits.

Glacier/snow pit	Al/Si	Rb/Sr	Sr/Ca	K/Ca	Fe/Ti
San Jose	0.8815	0.7028	0.0004	0.5161	0.3201
Whisky	0.6575	0.6112	0.0003	0.4633	0.2739
Triangular	0.2454	0.4309	0.0014	0.5995	3.9754
Davies Dome (top)	–	–	0.0003	0.5028	–
Davies Dome (down)	–	0.4249	0.0006	0.6386	5.8326

altitude/sediment deposition relationship determined for Whisky Glacier and Davies Dome. This suggests that in the case of Triangular Glacier, the local rock sources contribute more than 50% to the total HLD deposition on the surface. Whisky Glacier and Davies Dome (except for its lower parts) probably receive almost no local rock material because the upwind area of the southern Ulu Peninsula is almost completely glaciated.

The deposition rate on the studied glaciers of the Ulu Peninsula varies between 11.8 and 64 g m<sup>-2</sup>, which is one order higher than for other studied Antarctic glaciers. This is probably related to the local topography and the resulting available sources of material from the large ice-free area. Dunbar *et al.* (2009) observed a mean annual accumulation rate of 0.8 g m<sup>-2</sup> year<sup>-1</sup> on the McMurdo Ice Shelf. Lancaster (2002) reported a similar deposition rate on four glaciers in the McMurdo Dry Valleys (0.23–3.73 g m<sup>-2</sup> year<sup>-1</sup>), mostly composed of fine material of <50 μm. Chewings *et al.* (2014)

observed deposition rates varying between 0.2 and 55 g m<sup>-2</sup> year<sup>-1</sup> over the sea ice in McMurdo Sound. Arnalds *et al.* (2014) reported that the annual aeolian deposition rates in Iceland varied from a few grams per square metre per year up to 800 g m<sup>-2</sup> year<sup>-1</sup> with an estimate of 400 g m<sup>-2</sup> year<sup>-1</sup> deposition rate of volcanic dust on glacier surfaces. The annual deposition rate on Vatnajökull Glacier in Iceland was on the order of magnitude of 10–20 g m<sup>-2</sup> year<sup>-1</sup> (Wittmann *et al.*, 2017). Zdanowicz *et al.* (1998) identified a mean deposition rate of 0.48 g m<sup>-2</sup> year<sup>-1</sup> on Penny Ice Cap in Arctic Canada. Similar observations were reported from the subpolar or temperate climate, for example Owens and Slaymaker (1997) reported 13.1 g m<sup>-2</sup> year<sup>-1</sup> from British Columbia, Canada; Marx and McGowan (2005) observed deposition rates between 0.25 and 143 g m<sup>-2</sup> year<sup>-1</sup> in New Zealand. The deposition rate decreases significantly with altitude (e.g. Wittmann *et al.*, 2017), and with distance from the dust source (e.g. Arnalds *et al.*, 2014). Niveo-aeolian deposition was studied also by Ayling and McGowan (2006) in Victoria Valley. The snow pit sampling revealed a 35-year chronology of local aeolian depositions, which was apparent due to the different accumulation rates in the summer/winter parts of the year. In the case of the glaciers on the Ulu Peninsula, only one annual layer was identified.

As shown in Kavan *et al.* (2018), the local sources of aeolian material on the Ulu Peninsula are activated when the wind speed exceeds approximately 10 m s<sup>-1</sup>. Such a situation occurred in 7.8% of the studied time during the summer season of 2018. Similarly, Dunbar *et al.* (2009) reported a strong correlation between storminess (winds > 35 m s<sup>-1</sup>) and dust deposition rate on an ice shelf near McMurdo during the 35 years of recording. An important limiting factor for detachment of the local rock material from the surface is surface moisture (Wiggs *et al.*, 2004). Ground surface moisture gradually decreases during the summer season and the aeolian uplift is thus more likely to occur at the end of the summer season (Kavan *et al.*, 2018).

The idea of long-range material transport being the most important source for glacier surface deposition on the Ulu Peninsula is also supported by the relative amount of main and trace (mostly lithophile) elements, as seen for example in Figure 7, where the relation between altitude and main element contents is clearly visible. On the one hand, the strong negative correlation of proportions of Si, Ca and K with altitude suggests that the local sources play a more important role in the low-lying areas of the landscape. On the other hand, the effect of local rock material versus long-range transported material mostly sourced from the sea (marine aerosols) could be determined by the low Fe/Ti ratios, which are unprecedented in the geochemistry of the local bedrock (Figure 6). The transport of siliciclastic and partly calcareous sedimentary rocks of the Santa Marta

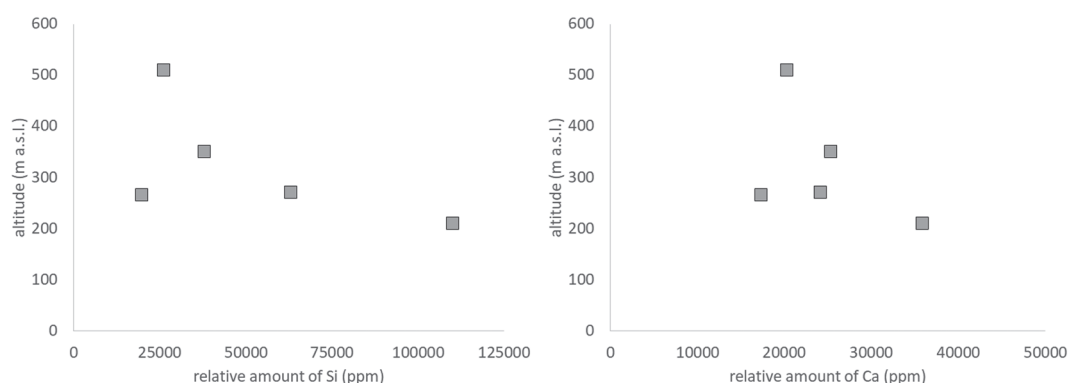


**Figure 7.** Relation between altitude and main element contents (Si, Ca).

Formation (Olivero *et al.*, 1986), cropping in the Abernethy Flats, to the surface of Triangular Glacier and partly also to the lower part of Davies Dome is reflected by high K/Ca ratios (Figure 6).

The lower Al/Si ratio indicates that much coarser aeolian material is deposited on Triangular Glacier if compared with the HLD deposited on San Jose and Whisky glaciers. The high Rb/Sr ratios (0.425–0.703) for all the HLD on the glaciers exclude the JRIVG rocks (Nelson, 1975) as the source material for aeolian transport on the glaciers. The Rb/Sr ratios of volcanic rocks lie in the range of 0.007–0.040 (Košler *et al.*, 2009; Altunkaynak *et al.*, 2018). Higher values are found in the sedimentary rocks of the Santa Marta Formation (0.235–0.300, see Figure 6). Furthermore, the K/Ca ratio is indicative for differentiation between Cretaceous and volcanic rock sources. The geochemical data reported by Košler *et al.* (2009) and Altunkaynak *et al.* (2018) show the K/Ca ratio being in the range 0.063–0.485, coinciding with our XRF-based K/Ca ratio of JRIVG basalts (0.040–0.355) and hyaloclastites (0.088–0.424). This is similar to the values calculated for aeolian deposition on the studied glaciers (0.463–0.639), but the samples from individual glaciers differ in Fe/Ti ratio, as can be seen in Figure 6. However, our calculated Rb/Sr and Fe/Ti ratio values (Figure 6) imply that the aeolian material deposited on Triangular Glacier and the lower part of Davies Dome is a mixture of local sedimentary rocks and marine aerosols.

In contrast, higher values of Rb/Sr ratios found for San Jose and Whisky glaciers and the top-site sample from Davies Dome correspond with long-range transport enriching the deposited material from the marine environment. This is also connected with Sr and Fe depletion in marine-sourced material when compared with geological material. Such material can be brought from HLD sources on the Antarctic Peninsula or even more distant sources. Fortner *et al.* (2011, 2013) identified aeolian deposition on glacier surfaces as a dominant process enriching the local freshwater ecosystems with trace elements.

A trajectory analysis showed the source areas for deposition at Syowa Station (located in Queen Maud Land, East Antarctica) being in South America and Africa, suggesting that long-range transport is not an exceptional event in Antarctica. Similarly, Patagonia was identified as a source area of dust deposition on the Ulu Peninsula during the 2018 summer season (Kavan *et al.*, 2018; Gassó and Torres, 2019). High concentration of Na and Cl was found from the injection of sea-salt particles during transport (Hara *et al.*, 2010). Lawrence *et al.* (2010) reported higher contents of Ca and K in snow samples with dust compared to snow without any apparent dust layers, suggesting the concentration of these elements is a useful proxy for the presence of atmospheric deposition. In accordance with the findings of Vallelonga *et al.* (2004) from Law Dome, Antarctica, a positive correlation ( $r^2 = 0.91$ ) between Ca–Sr concentrations in all the snow pit samples was found, suggesting that marine aerosols are the dominant sources of deposited material. The distance from the sea on Law Dome of about 100 km and the presence of no local dust sources in the vicinity clearly indicates the importance of long-range transport from distant sources, which could be valid for most sites in Antarctica.

Snow samples from distinct layers of the snow profile have been sampled in order to detect year-on-year variability in the concentration of main and trace elements. However, the rather heterogeneous vertical profiles (all but Davies top site – see Figure 4) of the snow pits only indicate a horizon rich in aeolian dust in the upper part of the profile. This spatial pattern in concentration corresponds well with the frequently reported findings (e.g. Drab *et al.*, 2002) describing typical year-on-year fluctuation in the concentration of main elements. This means

that samples from only a single year were available from all the snow pits, probably except the topmost snow profile from Davies Dome.

## Conclusions

HLD deposition and concentration of main and trace elements was examined on four glaciers on the Ulu Peninsula, James Ross Island. On this basis, important roles of short-distance and long-range sources of deposited material were identified. The spatial pattern was modified by the local topography and consequently by the prevailing local wind properties. San Jose Glacier received a relatively small amount of aeolian material ( $11.8 \text{ g m}^{-2}$ ), whereas Triangular Glacier exhibited more than double the deposition rate expected ( $64 \text{ g m}^{-2}$ ). Such a difference in deposition rate is a result of the specific location of each glacier with respect to the prevailing winds and position of local HLD sources. The most important local HLD source of about  $15 \text{ km}^2$  in the Abernethy Flats was identified and supported by means of the geochemical analyses. The deposition rate of tens of grams per square metre is approximately one order higher than that of most of the Antarctic sites. Aeolian deposition on glaciers can have a significant effect on the glacier itself (through albedo), on the chemistry of water streams originating from the melting of these glaciers and consequently on the ecosystem connected to these streams.

*Acknowledgements*—This work was supported by the Czech Science Foundation projects GC16-14122 J, GC20-20240S and Ministry of Education, Youth and Sports of the Czech Republic projects LM2015078, CZ.02.1.01/0.0/0.0/16\_013/0001708 and the Masaryk University project MUNI/A/1576/2018. We also appreciate the help of the staff of JGM Station. We would like to thank Steven Riley (Language Department, University of Economics, Prague) for language corrections.

## Data Availability Statement

The data sets used and/or analysed during the current study are available from the corresponding author on reasonable request.

## Conflict of Interest Statement

The authors declare that there is no conflict of interest that could be perceived as prejudicing the impartiality of the findings reported.

## References

- Altunkaynak S, Aldanmaz E, Güraslan IN, Caliskanoglu AZ, Ünal A, Nývlt D. 2018. Lithostratigraphy and petrology of Lachman Crags and Cape Lachman lava-fed deltas, Ulu Peninsula, James Ross Island, north-eastern Antarctic Peninsula: preliminary results. *Czech Polar Reports* **8**: 60–83.
- Arnalds O, Dagsson-Waldhauserova P, Olafsson H. 2016. The Icelandic volcanic aeolian environment: processes and impacts – a review. *Aeolian Research* **20**: 176–195.
- Arnalds O, Olafsson H, Dagsson-Waldhauserova P. 2014. Quantification of iron-rich volcanogenic dust emissions and deposition over the ocean from Icelandic dust sources. *Biogeosciences* **11**: 6623–6632.
- Arnalds O, Thorarinsdottir EF, Thorsson J, Dagsson-Waldhauserova P, Agustdottir AM. 2013. An extreme wind erosion event of the fresh Eyjafjallajökull 2010 volcanic ash. *Scientific Reports* **3**: 1257. <https://doi.org/10.1038/srep01257>.

- Atkins CB, Dunbar GB. 2009. Aeolian sediment flux from sea ice into southern McMurdo Sound, Antarctica. *Global Planetary Change* **69**: 133–141.
- Ayling BF, McGowan HA. 2006. Niveo-eolian sediment deposits in coastal south Victoria Land, Antarctica: indicators of regional variability in weather and climate. *Arctic, Antarctic, and Alpine Research* **38**: 313–324.
- Basile I, Grousset FE, Revel M, Petit JB, Biscaye PE, Barkov NI. 1997. Patagonian origin of glacial dust deposited in East Antarctica (Vostok and Dome C) during glacial stages 2, 4 and 6. *Earth and Planetary Science Letters* **146**: 573–589.
- Bory A, Wolff E, Mulvaney R, Jagoutz E, Wegner A, Ruth U, Elderfield H. 2010. Multiple sources supply eolian mineral dust to the Atlantic sector of coastal Antarctica: Evidence from recent snow layers at the top of Berkner Island ice sheet. *Earth and Planetary Science Letters* **291**: 138–148. <https://doi.org/10.1016/j.epsl.2010.01.006>
- Bullard JE. 2013. Contemporary glaciogenic inputs to the dust cycle. *Earth Surface Processes and Landforms* **3**: 71–89.
- Bullard JE, Austin MJ. 2011. Dust generation on a proglacial floodplain, West Greenland. *Aeolian Research* **3**: 43–54.
- Bullard JE, Baddock M, Bradwell T, Crusius J, Darlington E, Gaiero D, Gassó S, Gisladóttir G, Hodgkins R, McCulloch R, McKenna Neuman C, Mockford T, Stewart H, Thorsteinsson T. 2016. High-latitude dust in the Earth system. *Reviews of Geophysics* **54**: 447–485.
- Carrivick J, Davies B, Glasser N, Nývlt D, Hambrey M. 2012. Late-Holocene changes in character and behaviour of land-terminating glaciers on James Ross Island, Antarctica. *Journal of Glaciology* **58**: 1176–1190.
- Chewings JM, Atkins CB, Dunbar GB, Gollledge NR. 2014. Aeolian sediment transport and deposition in a modern high-latitude glacial marine environment. *Sedimentology* **61**: 1535–1557.
- Croft B, Martin RV, Leaitch WR, Tunved P, Breider TJ, D'Andrea SD, Pierce JR. 2016. Processes controlling the annual cycle of Arctic aerosol number and size distributions. *Atmospheric Chemistry and Physics* **16**: 3665–3682.
- Delmonte B, Basile-Doelsch I, Petit JR, Maggi V, Revel-Rolland M, Michard A, Jagoutz E, Grousset F. 2004. Comparing the Epica and Vostok dust records during the last 220,000 years: stratigraphical correlation and provenance in glacial periods. *Earth-Science Reviews* **66**: 63–87.
- Dixon DA, Mayewski PA, Korotkikh E, Sneed SB, Handley MJ, Introne DS, Scambos TA. 2013. Variations in snow and firn chemistry along US ITASE traverses and the effect of surface glazing. *The Cryosphere* **7**: 515–535.
- Drab E, Gaudichet A, Jaffrezo JL, Colin JL. 2002. Mineral particles content in recent snow at Summit Greenland. *Atmospheric Environment* **36**: 5365–5376.
- Dunbar GB, Bertler NAN, McKay RM. 2009. Sediment flux through the McMurdo Ice Shelf in Windless Bight, Antarctica. *Global and Planetary Change* **69**: 87–93.
- Engel Z, Láška K, Nývlt D, Stachoň Z. 2018. Surface mass balance of small glaciers on James Ross Island, north-eastern Antarctic Peninsula, during 2009–2015. *Journal of Glaciology* **64**: 349–361.
- Engel Z, Nývlt D, Láška K. 2012. Ice thickness, areal and volumetric changes of Davies Dome and Whisky Glacier, James Ross Island, Antarctic Peninsula in 1979–2006. *Journal of Glaciology* **58**: 904–914.
- Fischer H, Siggaard-Andersen ML, Ruth U, Rothlisberger R, Wolff E. 2007. Glacial/interglacial changes in mineral dust and sea-salt records in polar ice cores: sources, transport, and deposition. *Reviews of Geophysics* **45**: RG1002. <https://doi.org/10.1029/2005RG000192>
- Fortner SK, Lyons WB, Munk L. 2013. Diel stream geochemistry, Taylor Valley, Antarctica. *Hydrological Processes* **27**: 394–404.
- Fortner SK, Lyons WB, Olesik WB. 2011. Eolian deposition of trace elements onto Taylor Valley Antarctic glaciers. *Applied Geochemistry* **26**: 1897–1904.
- Gaiero DM. 2007. Dust provenance in Antarctic ice during glacial periods: from where in southern South America? *Geophysical Research Letters* **34**: L17707. <https://doi.org/10.1029/2007GL030520>
- Gassó S, Stein A, Marino F, Castellano E, Udisti R, Ceratto J. 2010. A combined observational and modeling approach to study modern dust transport from the Patagonia desert to East Antarctica. *Atmospheric Chemistry and Physics* **10**: 8287–8303.
- Gassó S, Torres O. 2019. Temporal characterization of dust activity in the Central Patagonia desert (years 1964–2017). *Journal of Geophysical Research: Atmospheres* **124**(6): 3417–3434.
- Gilli S, Gaiero DM, Goldstein SL, Chemale F, Koester E, Jweda J, Vallenga P, Kaplan MR. 2016. Provenance of dust to Antarctica: a lead isotopic perspective. *Geophysical Research Letters* **43**: 2291–2298.
- Hara K, Osada K, Yabuki M, Hashida G, Yamanouchi T, Hayashi M, Shiobara M, Nishita C, Wada M. 2010. Haze episodes at Syowa Station, coastal Antarctica: where did they come from? *Journal of Geophysical Research* **115**: D14205. <https://doi.org/10.1029/2009JD012582>
- Hedding DW, Nel W, Anderson RL. 2015. Aeolian processes and landforms in the sub-Antarctic: preliminary observations from Marion Island. *Polar Research* **34**: 26365. <https://doi.org/10.3402/polar.v34.26365>
- Kavan J, Dagsson-Waldhauserova P, Renard JB, Láška K, Ambrožová K. 2018. Aerosol concentrations in relationship to local atmospheric conditions on James Ross Island, Antarctica. *Frontiers in Earth Science* **6**. <https://doi.org/10.3389/feart.2018.00207>
- Kavan J, Nývlt D. 2018. Blowing in the wind – where does the Antarctic fluvial suspended load come from? In POLAR 2018: Where the Poles come together – Abstract Proceedings, Cambridge.
- Kavan J, Ondruch J, Nývlt D, Hrbáček F, Carrivick JL, Láška K. 2017. Seasonal hydrological and suspended sediment transport dynamics in proglacial streams, James Ross Island, Antarctica. *Geografiska Annaler: Series A, Physical Geography* **99**: 38–55.
- Křázková M, Hrbáček F, Kavan J, Nývlt D. 2020. Effect of hyaloclastite breccia boulders on meso-scale periglacial-aeolian landsystem in semi-arid Antarctic environment, James Ross Island, Antarctic Peninsula. *Cuadernos de Investigación Geográfica*. <https://doi.org/10.18172/cig.3800>
- Košler J, Magna T, Mlčoch B, Mixa P, Nývlt D, Holub FV. 2009. Combined Sr, Nd, Pb and Li isotope geochemistry of alkaline lavas from northern James Ross Island (Antarctic Peninsula) and implications for back-arc magma formation. *Chemical Geology* **258**: 207–218.
- Lancaster N. 2002. Flux of eolian sediment in the McMurdo Dry Valleys, Antarctica: a preliminary assessment. *Arctic, Antarctic and Alpine Research* **34**: 318–323.
- Láška K, Engel Z, Nývlt D, Stachoň Z, Lippel S, Braun M. 2017. Response of glacier mass on recent temperature cooling in northeastern Antarctic Peninsula. *Geophysical Research Abstracts* **19**: EGU2017–EGU2601.
- Lawrence CR, Neff JC. 2009. The contemporary physical and chemical flux of aeolian dust: a synthesis of direct measurements of dust deposition. *Chemical Geology* **267**: 46–63.
- Lawrence CR, Painter TH, Landry CC, Neff JC. 2010. Contemporary geochemical composition and flux of aeolian dust to the San Juan Mountains, Colorado, United States. *Journal of Geophysical Research* **115**: G03007. <https://doi.org/10.1029/2009JG001077>
- Legrand M, Preunkert S, Wolff E, Weller R, Jourdain B, Wagenbach D. 2017. Year-round records of bulk and size-segregated aerosol composition in central Antarctica (Concordia site) – part 1: fractionation of sea-salt particles. *Atmospheric Chemistry and Physics* **17**: 14039–14054.
- Marx SK, McGowan HA. 2005. Dust transportation and deposition in a superhumid environment, West Coast, South Island, New Zealand. *Catena* **59**: 147–171.
- Mlčoch B, Nývlt D, Mixa P (eds). 2018. *Geological map of James Ross Island – Northern part 1: 25,000*. Czech Geological Survey, Praha.
- Nelson PHH. 1975. The James Ross Island Volcanic Group of North–East Graham Land. *British Antarctic Survey Scientific Report* **54**: 62.
- Olivero EB, Scasso RA, Rinaldi CA. 1986. Revision of the Marambio Group, James Ross Island, Antarctica. *Contribuciones del Instituto Antártico Argentino* **331**: 1–28
- Owens PN, Slaymaker O. 1997. Contemporary and post-glacial rates of aeolian deposition in the Coast Mountains of British Columbia, Canada. *Geografiska Annaler, Series A: Physical Geography* **79**: 267–276.
- Pereira KCD, Evangelista H, Pereira EB, Simoes JC, Johnson E, Melo LR. 2004. Transport of crustal microparticles from Chilean Patagonia to

- the Antarctic Peninsula by SEM-EDS analysis. *Tellus B: Chemical and Physical Meteorology* **56**: 262–275.
- Rabassa J, Skvarca P, Bertani L, Mazzoni E. 1982. Glacier inventory of James Ross and Vega Islands, Antarctic Peninsula. *Annals of Glaciology* **3**: 260–264.
- Šabacká M, Priscu JC, Basagic HJ, Fountain AG, Wall DH, Virginia RA, Greenwood MC. 2012. Aeolian flux of biotic and abiotic material in Taylor Valley, Antarctica. *Geomorphology* **155–156**: 102–111.
- Selby MJ, Rains RB, Palmer RWP. 1974. Eolian deposits of the ice-free Victoria Valley, Southern Victoria Land, Antarctica. *New Zealand Journal of Geology and Geophysics* **17**: 543–562.
- Speirs JC, McGowan HA, Neil DT. 2008. Polar eolian sand transport: grain characteristics determined by an automated scanning electron microscope QEMSCANHH. *Arctic, Antarctic and Alpine Research* **40**: 731–743.
- Vallelonga P, Barbante C, Cozzi G, Gaspari V, Candelone J, Van de Velde K, Morgan VI, Rosman KJR, Boutron CF, Cescon P. 2004. Elemental indicators of natural and anthropogenic aerosol inputs to Law Dome, Antarctica. *Annals of Glaciology* **39**: 169–134.
- Weller R, Minikin A, Petzold A, Wagenbach D, König-Langlo G. 2013. Characterization of long-term and seasonal variations of black carbon (BC) concentrations at Neumayer, Antarctica. *Atmospheric Chemistry and Physics* **13**: 1579–1590.
- Weller R, Woltjen J, Piel C, Resenberg R, Wagenbach D, König-Langlo G, Kriews M. 2008. Seasonal variability of crustal and marine trace elements in the aerosol at Neumayer station, Antarctica. *Tellus B: Chemical and Physical Meteorology* **60**: 742–752.
- Wiggs G, Baird A, Atherton R. 2004. The dynamic effects of moisture on the entrainment and transport of sand by wind. *Geomorphology* **59**: 13–30.
- Wittmann M, Groot Zwaafink CD, Steffensen Schmidt L, Guðmundsson S, Pálsson F, Arnalds O, Björnsson H, Thorsteinsson T, Stohl A. 2017. Impact of dust deposition on the albedo of Vatnajökull ice cap, Iceland. *The Cryosphere* **11**: 741–754.
- Zdanowicz CM, Zielinski GA, Wake CP. 1998. Characteristics of modern atmospheric dust deposition in snow on the Penny Ice Cap, Baffin Island, Arctic Canada. *Tellus, Series B: Chemical and Physical Meteorology* **50**: 506–520.